

The NEXT experiment: status and prospects

The NEXT collaboration

A. Introduction

Neutrinos, unlike the other fermions of the Standard Model of particle physics, could be Majorana particles, that is, indistinguishable from their antiparticles. The existence of Majorana neutrinos would have profound implications in particle physics and cosmology.

If neutrinos are Majorana particles, there must exist a new scale of physics (at a level inversely proportional to the neutrino masses) that characterises the underlying dynamics beyond the Standard Model. The existence of such a new scale provides the simplest explanation of why neutrino masses are so much lighter than the charged fermions. Indeed, understanding the new physics responsible for neutrino masses is one of the most important open questions in particle physics, and could have profound implications in our comprehension of the mechanism of symmetry breaking, the origin of mass and the flavour problem.

The discovery of Majorana neutrinos would also mean that total lepton number is not conserved, an observation that could be linked to the origin of the matter-antimatter asymmetry observed in the Universe today. This is because the new physics responsible for neutrino masses could provide a new mechanism to generate this asymmetry, via a process called leptogenesis. Although the predictions are model dependent, two essential ingredients must be confirmed experimentally for leptogenesis to occur: 1) the violation of lepton number and 2) CP violation in the lepton sector.

The only practical way to establish experimentally whether neutrinos are their own antiparticles, and whether lepton number is not conserved, is the detection of neutrinoless double beta decay ($\beta\beta 0\nu$). This is a hypothetical, very slow nuclear transition in which a nucleus with Z protons decays into a nucleus with $Z + 2$ protons and the same mass number A , emitting two electrons that carry essentially all the energy released ($Q_{\beta\beta}$). The process can occur if and only if neutrinos are Majorana particles.

A.1. The experimental landscape

The detectors used in double beta decay searches are designed to measure the energy of the radiation emitted by a $\beta\beta$ source. In the case of $\beta\beta 0\nu$, the sum of the kinetic energies of the two released electrons is fixed by the mass difference between the parent and the daughter nuclei: $Q_{\beta\beta} \equiv M(Z, A) - M(Z + 2, A)$. However, due to the finite energy resolution of any detector, $\beta\beta 0\nu$ events are reconstructed within an energy region centered around $Q_{\beta\beta}$, typically following a gaussian distribution (Region of Interest, or ROI). Other processes occurring in the detector can fall in the ROI, becoming a background and compromising drastically the expected sensitivity. It follows that $\beta\beta 0\nu$ experiments require **excellent energy resolution**, and indeed the field has been traditionally dominated by germanium calorimeters, devices with superb resolution.

All double beta decay experiments have to deal with an intrinsic background, the $\beta\beta 2\nu$, the standard process of a double β -decay with the emission of two neutrinos, that can only be suppressed by means of good energy resolution. Backgrounds of cosmogenic origin force the **underground operation of the detectors**. Natural radioactivity emanating from the detector materials and surroundings can easily overwhelm the signal peak, and hence **careful selection of radiopure materials is also essential**. **Additional experimental signatures** that allow the distinction between signal and background are certainly a bonus, and this has been in the last few years an important line of work to increase the sensitivity of $\beta\beta 0\nu$ detectors. Several other factors such as **detection efficiency** or the **scalability to large masses** must also be taken into account during the design of a double beta decay experiment.

A.2. Recent results

Three new-generation experiments, with fiducial masses in the range of 100 kg, have recently published the results of their searches for $\beta\beta 0\nu$ processes. These are: GERDA, a high resolution calorimeter based on ^{76}Ge diodes; KamLAND-Zen, a low resolution, high-mass, self-shielding liquid scintillator calorimeter, with xenon dissolved in the scintillator; and EXO-200, a liquid xenon (LXe) TPC. All the experiments

published null results and therefore a lower limit on the period of $\beta\beta 0\nu$ processes, $T_{1/2}^{0\nu}$. This lower limit can be translated into an upper limit on the *effective Majorana mass* of the electron neutrino defined as:

$$m_{\beta\beta} = \left| \sum_i U_{ei}^2 m_i \right|, \quad (1)$$

where m_i are the neutrino mass eigenstates and U_{ei} are elements of the neutrino mixing matrix. The mass $m_{\beta\beta}$ is related to the period through the equation:

$$(T_{1/2}^{0\nu})^{-1} = G^{0\nu} |M^{0\nu}|^2 m_{\beta\beta}^2. \quad (2)$$

In Eq. 2, $G^{0\nu}$ is an exactly-calculable phase-space integral for the emission of two electrons and $M^{0\nu}$ is the nuclear matrix element (NME) of the transition, which has to be evaluated theoretically. The uncertainty in the NME affects the value of $m_{\beta\beta}$ which can be obtained from $T_{1/2}^{0\nu}$.

GERDA¹ has a resolution of $\sim 0.2\%$ FWHM around the $Q_{\beta\beta}$ of ^{76}Ge . The specific background rate in the ROI is 10^{-2} counts/(keV · kg · yr) and the total exposure deployed is 21.6 kg·yr. The experiment sets a limit $T_{1/2}^{0\nu}(^{76}\text{Ge}) > 2 \times 10^{25}$ yr, which translates into an upper limit range for $m_{\beta\beta}$ of [258 – 649] milli electronvolts (meV). The lowest value of the $m_{\beta\beta}$ upper limit corresponds to the IBM2 NME set², while the highest value corresponds to the ISM set³.

EXO⁴ achieves an energy resolution of 3.6% FWHM at $Q_{\beta\beta}$, and a background rate of 4×10^{-3} counts/(keV · kg · yr). The total exposure used for the published result is 100 kg · yr. The EXO Collaboration has published a limit on the half-life of $\beta\beta 0\nu$ in ^{136}Xe of $T_{1/2}^{0\nu}(^{136}\text{Xe}) > 2 \times 10^{25}$ yr. The limit translates into an upper limit range for $m_{\beta\beta}$ of [125 – 352] meV, depending on the NME.

KamLAND-Zen⁵ compensates a worse energy resolution of 10% FWHM at $Q_{\beta\beta}$ with a very small background rate of $\sim 4 \times 10^{-4}$ counts/(keV · kg · yr). After an exposure of 108.8 kg · yr, they obtain a limit $T_{1/2}^{0\nu}(^{136}\text{Xe}) > 2,6 \times 10^{25}$ yr, which translates into an upper limit range for $m_{\beta\beta}$ of [110 – 309] meV, depending on the NME.

A.3. Potential for discovery

Several analyses from recent cosmological results suggest that the sum of the masses of the three neutrinos could be ~ 0.3 eV⁶. In this case, if the neutrino is a Majorana particle, then, $m_{\beta\beta} \sim [20 – 150]$ meV⁷, as shown in Figure 1. In this scenario, the sensitivity of GERDA is outside the “cosmologically relevant region” (CRR), while both EXO-200 and KamLAND-Zen would have already explored a significant fraction of CRR *for the most optimistic NME set* (while they would be outside CRR for the most pessimistic).

Clearly, the experimental effort to determine if the neutrino is a Majorana particle, far from being completed is, rather, in its infancy. To establish unambiguously that the neutrino is (or not) a Majorana particle, even in this favourable scenario in which the sum of the neutrino masses is relatively high, experiments must be sensitive to $m_{\beta\beta} \sim 20$ meV, *even for the most pessimistic NME set*. This is a major challenge.

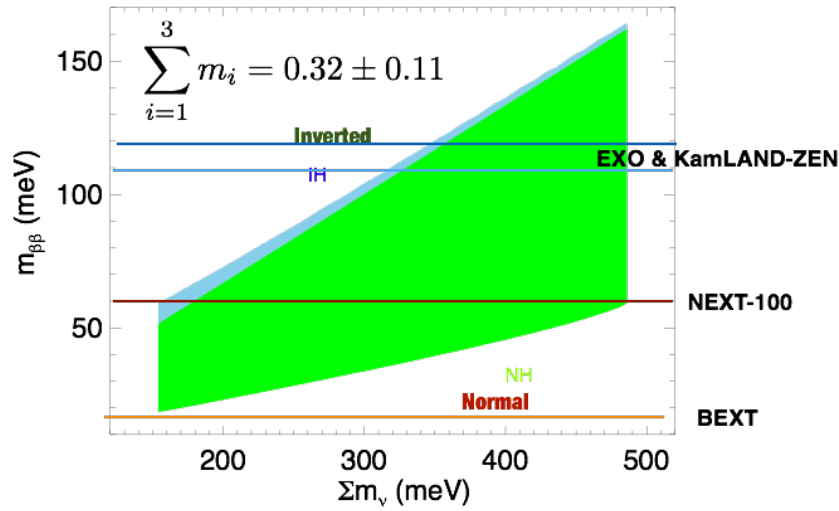


Figure 1: The allowed $m_{\beta\beta}$ region (68% CL for two degrees of freedom), as a function of the sum of the neutrino masses, assuming that $\sum m_i = 0,32 \pm 0,11$ eV. The blue lines mark the sensitivity of EXO and KamLAND-ZEN, the xenon-based detectors currently leading the field. The red line shows the sensitivity of NEXT after 3 years operation, which gives the experiment a sizable chance of making a discovery.

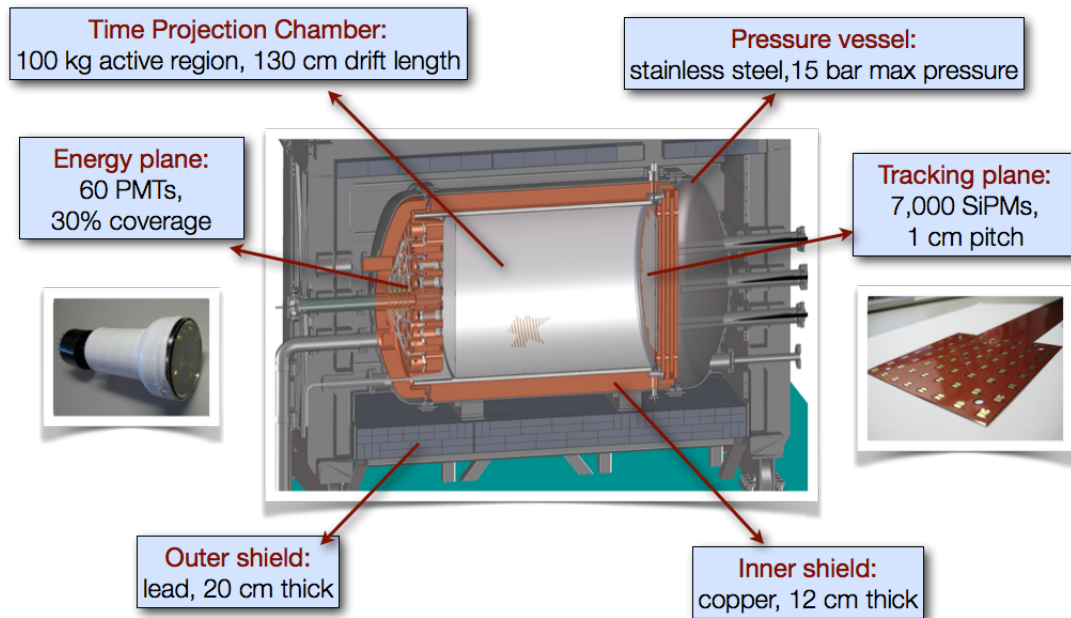


Figure 2: A drawing of the NEXT-100 detector showing its main parts. The pressure vessel (PV) is made of a radio pure steel-titanium alloy. The PV dimensions are 130 cm inner diameter, 222 cm length, 1 cm thick walls, for a total mass of 1 200 kg. The inner copper shield (ICS) is made of ultra-pure copper bars and is 12 cm thick, with a total mass of 9 000 kg. The time projection chamber includes the field cage, cathode, EL grids and HV penetrators. The light tube is made of thin teflon sheets coated with TPB (a wavelength shifter). The energy plane is made of 60 PMTs housed in copper enclosures (cans). The tracking plane is made of MPPCs arranged into dice boards (DB).

B. The NEXT experiment and its innovative concepts

The *Neutrino Experiment with a Xenon TPC* (NEXT)⁸ will search for $\beta\beta 0\nu$ in ^{136}Xe using high-pressure xenon gas time projection chambers (HPXE)⁹, yielding: a) **excellent energy resolution**, with an intrinsic limit of about 0.3% FWHM at $Q_{\beta\beta}$, and close to that of ^{76}Ge detectors and a demonstrated result in the vicinity of 0.5% FWHM; b) **tracking capabilities** that provide a powerful topological signature to discriminate between signal (two electron tracks with a common vertex) and background (mostly, single electrons); c) **a fully active and homogeneous detector**, with no dead regions; d) **scalability** of the technique to large masses; e) the possibility of exciting the barium ion produced in the xenon decay from the fundamental state $^2S_{1/2}$ to the state $^2P_{1/2}$, using a “blue” laser (493.54 nm), and observing the “red light” emitted in the transition from $^2P_{1/2}$ to $^2D_{3/2}$, thus “tagging” the presence of a barium atom in the xenon gas, which cannot be produced by any known background.

The design of the NEXT-100 detector (Figure 2) is optimised for energy resolution by using proportional electroluminescent (EL) amplification of the ionisation signal¹⁰. The detection process involves the use of the prompt scintillation light from the gas as start-of-event time, and the drift of the ionisation charge to the anode by means of an electric field ($\sim 0,3$ kV/cm at 15 bar) where secondary EL scintillation is produced in the region defined by two highly transparent meshes, between which there is a field of ~ 20 kV/cm at 15 bar. The detection of EL light provides an energy measurement using photomultipliers (PMTs) located behind the cathode (the *energy plane*) as well as tracking through its detection a few mm away from production at the anode, via a dense array of silicon photomultipliers (the *tracking plane*).

B.1. NEXT prototypes

NEXT-DEMO, shown in figure 3, is as a large-scale prototype of NEXT-100. The pressure vessel has a length of 60 cm and a diameter of 30 cm. The vessel can withstand a pressure of up to 15 bar and hosts typically 1-2 kg of xenon. NEXT-DEMO is equipped with an energy plane made of 19 Hamamatsu R7378A PMTs and a tracking plane made of 256 Hamamatsu SiPMs.

The detector has been operating successfully for more than two years and has demonstrated: (a) very good operational stability, with no leaks and very few sparks; (b) good energy resolution ; (c) track reconstruction with PMTs and with SiPMs coated with TPB; (d) excellent electron drift lifetime, of the order of 20 ms. Its construction, commissioning and operation has been instrumental in the development of the required knowledge to design and build the NEXT detector.

The NEXT-DBDM prototype (Figure 4) is a smaller chamber, with only 8 cm drift, but an aspect ratio (ratio diameter to length) similar to that of NEXT-100. The device has been used to perform detailed energy resolution studies, as well as studies to characterise neutrons in an HPXE. NEXT-DBDM achieves a resolution of 1% FWHM at 660 keV and 15 bar, which extrapolates to 0.5% at $Q_{\beta\beta}$.

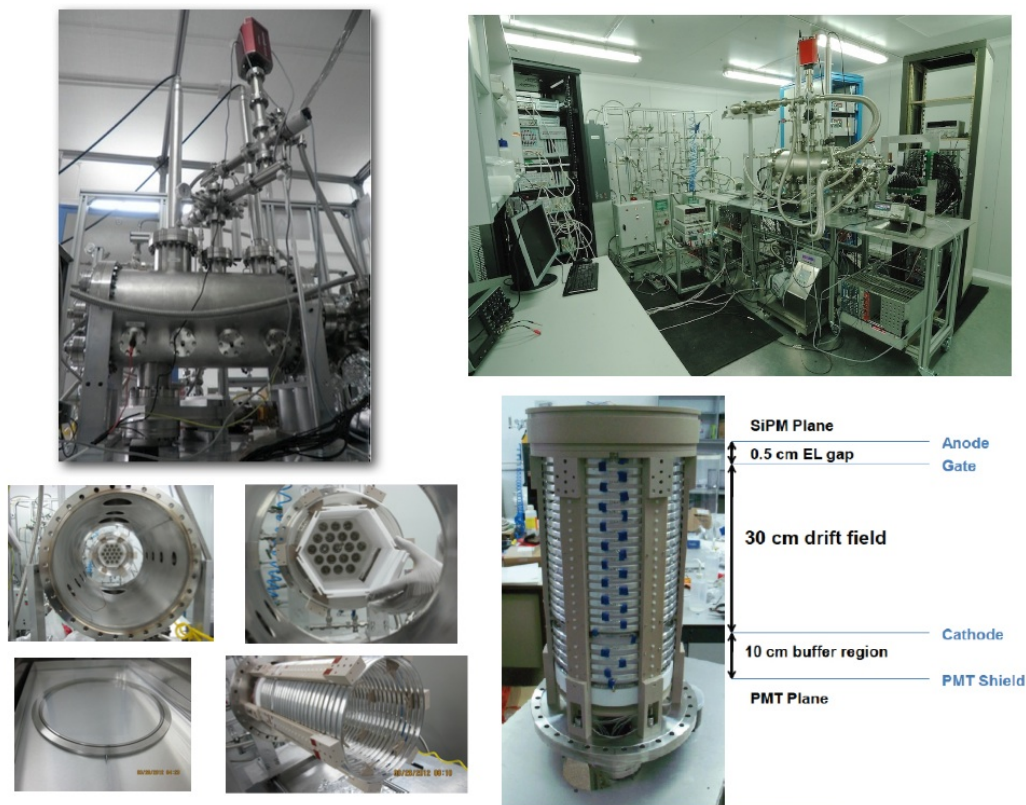


Figura 3: The NEXT-DEMO prototype. Top-left: the pressure vessel, showing the HVFT and the mass spectrometer; bottom-left: an expanded view of the detector; (c) Teflon light tube; (d) energy plane, made of pressure resistant Hamamatsu R7378A PMTs; (e) field cage; (f) tracking plane equipped with 300 Hamamatsu MPPCs; top-right: the full setup at IFIC; bottom right: the field cage.

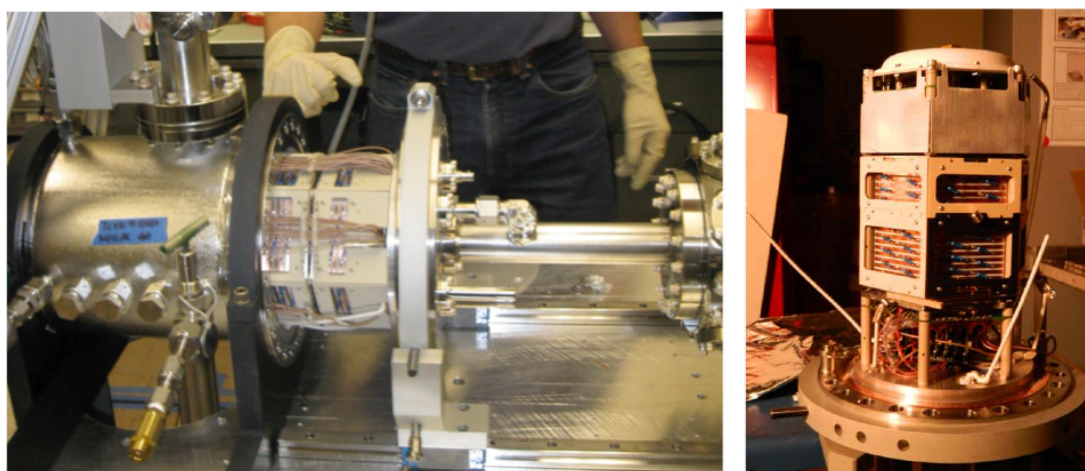


Figura 4: The NEXT-DBDM prototype. Top-left: the pressure vessel, in the moment in which the field cage is inserted; (b) the field cage.

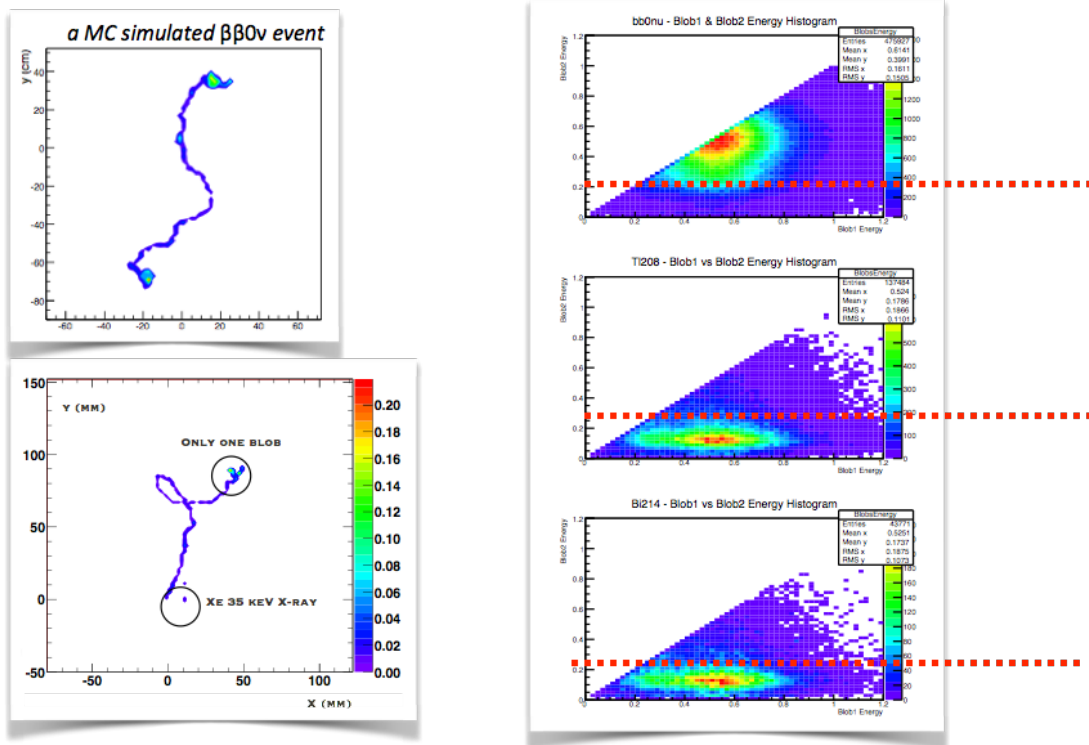


Figure 5: NEXt has a topological signature, not available in most $\beta\beta$ detectors. The panel shows the reconstruction of a Monte Carlo signal (topleft) and background (bottomleft) event. The signal has two electrons (two blobs). The background has only one electron (one blob) and the associated emission of a 35 keV X-ray. The color codes energy deposition in the TPC. An scatter plot of the energy of the two blobs shows a clear separation between signal and background regions.

Na22 high energy gamma - data from run 3200 vs reco MC

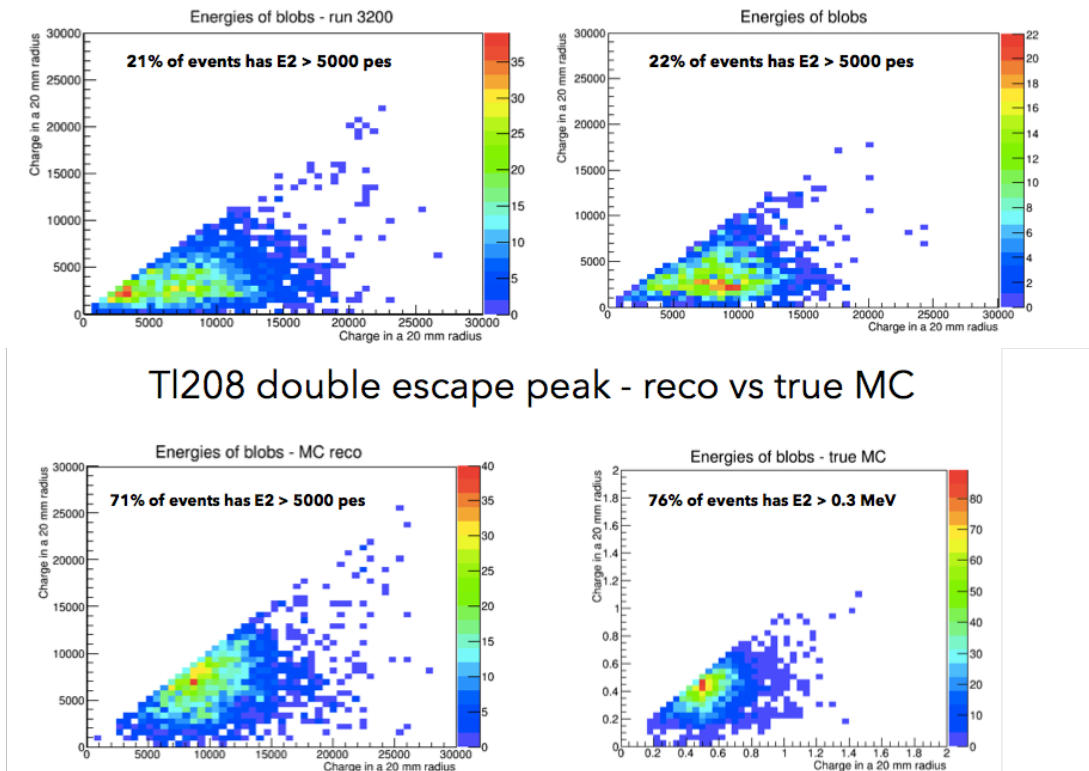


Figure 6: A comparison between data (left) and Monte Carlo (right) for electrons of different energies recorded in the DEMO chambers, showing the very good agreement between both data sets and therefore the robustness of the topological signal, unique of the NEXt experiment.

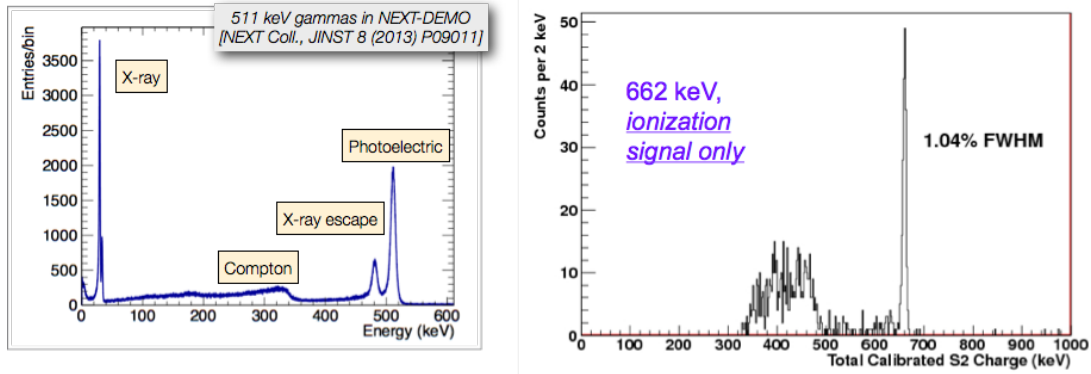


Figura 7: Left: the full energy spectrum measured for electrons of 511 keV in the DEMO detector. Right the spectrum near the photoelectric peak for 662 keV electrons in NEXT-DBDM. The resolution at 662 keV is 1% FWHM (0.5% FWHM at $Q_{\beta\beta}$). The resolution extrapolated from 511 keV is 0.7%.

B.2. Topological signature

Double beta decay events leave a distinctive topological signature in HPXe: a continuous track with larger energy depositions (*blobs*) at both ends due to the Bragg-like peaks in the dE/dx of the stopping electrons (figure 5, topleft). In contrast, background electrons are produced by Compton or photoelectric interactions, and are characterised by a single blob and, often, by a satellite cluster corresponding to the emission of ~ 30 -keV fluorescence x-rays by xenon (figure 5, bottomleft). Reconstruction of this topology using the tracking plane provides a powerful means of background rejection, as can be observed in the figure. In our TDR we chose a conservative cut to separate double-blob from single-blob events which provided a suppression factor of 20 for the background while keeping 80% of the signal. DEMO has reconstructed single electrons from ^{22}Na and ^{137}Cs sources, as well as double electrons from the double escape peak of ^{208}Tl demonstrating the robustness of the topological signal.

Figure 6 shows a comparison between data and Monte Carlo for electrons interacting in the DEMO detector. Two radioactive sources were used: Na-22, producing single electrons of 511 keV, and Tl-208, whose double escape peak produced *double electrons*, at the energy of 1.6 MeV. Both data sets allow us to “mimic” signal and background and thus have a robust assessment of the performance of the topological signal comparing the Monte Carlo simulation and the actual results obtained with DEMO. The agreement between both data sets is very good, revealing the robustness of the topological signal.

B.3. Energy resolution

Figure 7 shows the resolution obtained with the NEXT-DBDM apparatus. A resolution of 1% FWHM with 662 keV photons, has been measured, which extrapolates to 0.5% FWHM at $Q_{\beta\beta}$. This result is

¹M. Agostini y col. “Results on Neutrinoless Double- β Decay of ^{76}Ge from Phase I of the GERDA Experiment”. En: *Phys.Rev.Lett.* 111.12 (2013), pág. 122503. arXiv: 1307.4720 [nucl-ex].

²J. Barea, J. Kotila y F. Iachello. “Nuclear matrix elements for double- β decay”. En: *Phys.Rev.* C87 (2013), pág. 014315. arXiv: 1301.4203 [nucl-th].

³J. Menendez y col. “Disassembling the Nuclear Matrix Elements of the Neutrinoless beta beta Decay”. En: *Nucl.Phys.* A818 (2009), págs. 139-151. arXiv: 0801.3760 [nucl-th].

⁴J.B. Albert y col. “Search for Majorana neutrinos with the first two years of EXO-200 data”. En: *Nature* 510 (2014), 229–234. arXiv: 1402.6956 [nucl-ex].

⁵“Results from KamLAND-Zen”. En: (2014). arXiv: 1409.0077 [physics.ins-det].

⁶Richard A. Battye y Adam Moss. “Evidence for Massive Neutrinos from Cosmic Microwave Background and Lensing Observations”. En: *Phys. Rev. Lett.* 112 (5 2014), pág. 051303. URL: <http://link.aps.org/doi/10.1103/PhysRevLett.112.051303>.

⁷J.J. Gómez-Cadenas y col. “Discovery potential of xenon-based neutrinoless double beta decay experiments in light of small angular scale CMB observations”. En: *JCAP* 1303 (2013), pág. 043. arXiv: 1301.2901 [hep-ph].

⁸URL: <http://next.ific.uv.es/>.

⁹V. Alvarez y col. “NEXT-100 Technical Design Report (TDR): Executive Summary”. En: *JINST* 7 (2012), T06001. arXiv: 1202.0721 [physics.ins-det]; F. Granena y col. “NEXT, a HPGXe TPC for neutrinoless double beta decay searches”. En: (2009). arXiv: 0907.4054 [hep-ex]; David Nygren. “High-pressure xenon gas electroluminescent TPC for $0\nu\beta\beta$ search”. En: *Nucl.Instrum.Meth.* A603 (2009), págs. 337-348.

¹⁰As proposed in (Nygren, [seemote 9](#))

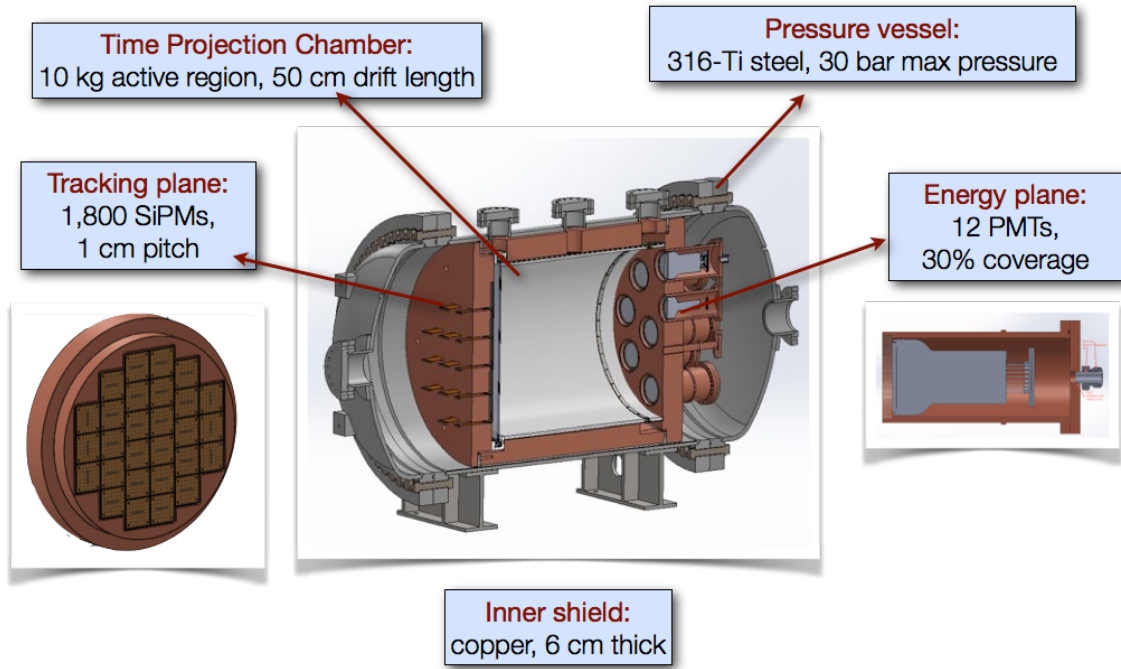


Figura 8: The NEW apparatus.

not far from the expected limit obtained adding in quadrature the different factors that contribute to the resolution (Fano factor, photoelectron statistics and electronic noise). The resolution measured in NEXT-DEMO extrapolates to 0.7% FWHM. The difference between both prototypes is due to better photoelectron statistics and aspect ratio in DBDM. The results, are, in any case, better than the target of 1% FWHM described in the TDR.

The status of the NEXT experiment and the results achieved by the prototypes have been described in a recent paper¹¹.

B.4. The NEW detector.

The NEW (NEXT-WHITE) apparatus¹², shown in Figure 8, is the first phase of the NEXT detector to operate underground. NEW is a scale 1:2 in size (1:8 in mass) of NEXT-100. The energy plane contains 12 PMTs (20% of the 60 PMTs deployed in NEXT-100). The tracking plane technology consists of 30 Kapton Dice Boards (KDB) deploying 1800 SiPMs (also 20% of the sensors). The field cage has a diameter of 50 cm and a length of 60 cm (the dimensions of the NEXT-100 field cage are roughly 1 m long and 1.2 m diameter).

NEW is a necessary step¹³ towards the construction of NEXT-100. It will validate the technological solutions adopted by the collaboration and, as discussed below, it is essential in the definition of the project methodology. Furthermore, The NEXT background model is currently based on a sophisticated Monte Carlo simulation of all expected background sources in each part of the detector. NEW will allow the validation of the background model with actual data.

Furthermore, the calibration of NEW with sources of higher energy, will allow a precise study of the evolution of the resolution with the energy. In particular it will be plausible to measure the resolution near $Q_{\beta\beta}$ using a Thorium source, which provides 2.6 MeV gammas. Last, but not least, we intend to reconstruct the spectrum of $\beta\beta 2\nu$. Those events are topologically identical to signal events ($\beta\beta 0\nu$) and can be used to demonstrate with data the power of the topological signature.

¹¹J.J. Gomez-Cadenas y col. "Present status and future perspectives of the NEXT experiment". En: (2013). arXiv: 1307.3914 [physics.ins-det].

¹²The name honours the memory of the late Professor James White, one of the key scientists of the NEXT Collaboration.

¹³As formally stated by the scientific committee of the LSC, who recommended its construction in 2013.

C. NEXT background model and expected sensitivity

The NEXT background model describes the sources of radioactive contaminants in the detector and their activity. It allows us, via detailed simulation, to predict the background events that can be misidentified as signal and consequently, to predict the expected sensitivity of the apparatus. A major goal of NEW is to confirm these predictions from the data themselves

C.1. Sources of background

Radioactive contaminants in detector materials

After the decay of ^{214}Bi , the daughter isotope, ^{214}Po , emits a number of de-excitation gammas with energies above 2.3 MeV. The gamma line at 2447 keV, of intensity 1.57%, is very close to the Q -value of ^{136}Xe . The gamma lines above $Q_{\beta\beta}$ have low intensity and their contribution is negligible.

The daughter of ^{208}Tl , ^{208}Pb , emits a de-excitation photon of 2614 keV with a 100% intensity. The Compton edge of this gamma is at 2382 keV, well below $Q_{\beta\beta}$. However, the scattered gamma can interact and produce other electron tracks close enough to the initial Compton electron so they are reconstructed as a single object falling in the energy region of interest (ROI). Photoelectric electrons are produced above the ROI but can lose energy via bremsstrahlung and populate the window, in case the emitted photons escape out of the detector. Pair-creation events are not able to produce single-track events in the ROI.

Radon

Radon constitutes a dangerous source of background due to the radioactive isotopes ^{222}Rn (half-life of 3.8 d) from the ^{238}U chain and ^{220}Rn (half-life of 55 s) from the ^{232}Th chain. As a gas, it diffuses into the air and can enter the detector. ^{214}Bi is a decay product of ^{222}Rn , and ^{208}Tl a decay product of ^{220}Rn . In both cases, radon undergoes an alpha decay into polonium, producing a positively charged ion which is drifted towards the cathode by the electric field of the TPC. As a consequence, ^{214}Bi and ^{208}Tl contaminations can be assumed to be deposited on the cathode surface. Radon may be eliminated from the TPC gas mixture by recirculation through appropriate filters. There are also ways to suppress radon in the volume defined by the shielding. Radon control is a major task for a $\beta\beta 0\nu$ experiment, and will be of uppermost importance for NEXT-100. A major goal of NEW is to assess (and eventually improve) the effectiveness of radon control techniques.

Cosmic rays and laboratory rock backgrounds

Cosmic particles can also affect our experiment by producing high energy photons or activating materials. This is the reason why double beta decay experiments are conducted deep underground. At these depths, muons are the only surviving cosmic ray particles, but their interactions with the rock produce neutrons and electromagnetic showers. Furthermore, the rock of the laboratory itself is a rather intense source of ^{208}Tl and ^{214}Bi backgrounds as well as neutrons.

The flux of photons emanating from the LSC walls is (see our TDR and references therein):

- $0,71 \pm 0,12 \text{ } \gamma/\text{cm}^2/\text{s}$ from the ^{238}U chain.
- $0,85 \pm 0,07 \text{ } \gamma/\text{cm}^2/\text{s}$ from the ^{232}Th chain.

These measurements include all the emissions in each chain. The flux corresponding to the ^{208}Tl line at 2614.5 keV and the flux corresponding to the ^{214}Bi line at 1764.5 keV were also measured (from the latter it is possible to deduce the flux corresponding to the 2448 keV line). The results are:

- $0,13 \pm 0,01 \text{ } \gamma/\text{cm}^2/\text{s}$ from the ^{208}Tl line.
- $0,006 \pm 0,001 \text{ } \gamma/\text{cm}^2/\text{s}$ from the ^{214}Bi line at 2448 keV.

The above backgrounds are considerably reduced by the shielding. In addition, given the topological capabilities of NEXT, the residual muon and neutron background do not appear to be significant for our experiment.

Cuadro 1: Activity (in mBq/kg) of the most relevant materials used in NEXT.

Material	Subsystem	^{238}U	^{232}Th	Ref.
Lead	Shielding	0.37	0.07	¹⁶
Copper	ICS	< 0,012	< 0,004	¹⁷
Steel (316Ti)	PV	< 0,57	< 0,54	¹⁸
Polyethylene	FC	0.23	< 0,14	¹⁹
PMT (R11410-MOD per pc)	EP	< 2,5	< 2,5	²⁰

Cuadro 2: Acceptance of the selection cuts for signal and backgrounds.

Selection cut	$\beta\beta 0\nu$	Fraction of events	
		^{214}Bi	^{208}Tl
Confined, single track	0.48	$6,0 \times 10^{-5}$	$2,4 \times 10^{-3}$
Energy ROI	0.33	$2,2 \times 10^{-6}$	$1,9 \times 10^{-6}$
Topology $\beta\beta 0\nu$	0.25	$1,9 \times 10^{-7}$	$1,8 \times 10^{-7}$

C.2. Radioactive budget of NEXT-100

Information on the radiopurity of the materials expected to be used in the construction of NEXT-100 has been compiled, performing specific measurements and also examining data from the literature for materials not yet screened. A detailed description is presented in¹⁴. A brief summary of the results presented there for the main materials is shown in Table 1¹⁵

C.3. Expected background rate

The only relevant backgrounds for NEXT are the photons emitted by the ^{208}Tl line (2614.5 keV) and the ^{214}Bi line (2448 keV). These sit very near $Q_{\beta\beta}$ and the interaction of the photons in the gas can fake the $\beta\beta 0\nu$ signal. NEXT-100 has the structure of a Matryoshka (a Russian nesting doll). The flux of gammas emanating from the LSC walls is drastically attenuated by the lead castle, and the residual flux, together with that emitted by the lead castle itself and the materials of the pressure vessel is further attenuated by the inner copper shielding. One then needs to add the contributions of the “inner elements” in NEXT: field cage, energy plane, and the elements of the tracking plane not shielded by the ICS.

A detailed Geant4²¹ simulation of the NEXT-100 detector was written in order to compute the background rejection factor achievable with the detector. Simulated events, after reconstruction, were accepted as a $\beta\beta 0\nu$ candidate if

- they were reconstructed as a single track confined within the active volume;
- their energy fell in the region of interest, defined as $\pm 0,5$ FWHM around $Q_{\beta\beta}$;
- the spatial pattern of energy deposition corresponded to that of a $\beta\beta 0\nu$ track (*blobs* in both ends).

The achieved background rejection factor together with the selection efficiency for the signal are shown in Table 2. As can be seen, the cuts suppress the radioactive background by more than 7 orders of magnitude. This results in an estimated background rate of about 4×10^{-4} counts/(keV · kg · yr).

¹⁴V. Alvarez y col. “Radiopurity control in the NEXT-100 double beta decay experiment: procedures and initial measurements”. En: (2012). arXiv: 1211.3961 [physics.ins-det].

¹⁵ICS means Internal Copper Shield; PV refers to the pressure vessel; FC to the field cage and EP to the energy plane.

²¹S. Agostinelli y col. “Geant4 simulation toolkit”. En: *Nuclear Instruments and Methods in Physics Research Section A: Accelerators, Spectrometers, Detectors and Associated Equipment* 506.3 (2003), págs. 250 -303. ISSN: 0168-9002. URL: <http://www.sciencedirect.com/science/article/pii/S0168900203013688>.

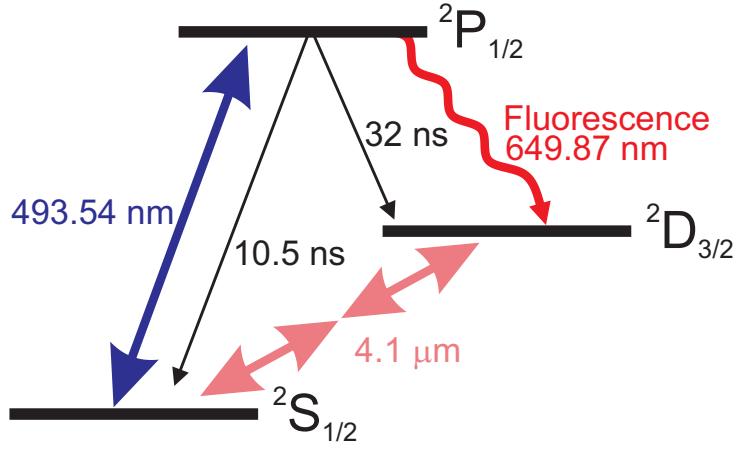


Figura 9: The BATA concept.

C.4. Discovery potential of NEXT-100.

The excellent resolution of NEXT (0.5% FWHM), and the combination of a low radioactive budget with a topological signature (which yields an expected background rate of 4×10^{-4} counts/(keV · kg · yr)), will allow the NEXT-100 detector to reach a sensitivity to the $\beta\beta 0\nu$ period of $T_{1/2}^{0\nu} > 7 \times 10^{25}$ yr for an exposure of 300 kg·yr. This translates into a $m_{\beta\beta}$ sensitivity range as low as [67 – 187] meV, depending on the NME. Therefore NEXT-100 will have a substantial chance of making a discovery if the NME is sufficiently high (see Fig. 1).

D. Towards a ton-scale high-pressure xenon TPC.

If no discovery is made by the current generation of experiments, the full exploration of the CRR region (corresponding to the inverted hierarchy of neutrino masses, and $m_{\beta\beta}$ values as low as 15 meV) requires detectors of larger mass (at least 1 ton), good resolution and extremely low specific background. The HPXE technology has the potential to provide the most sensitive detector at this scale, by scaling the detector to a mass in the range of one ton and adding additional handles to further suppress the background.

D.1. Adding a magnetic field to enhance the topological signal

The NEXT topological signal is based in the fact that single electrons (background events, produced by photoelectric and Compton interactions of high-energy gammas arising mostly from ^{214}Bi and ^{208}Tl) can be separated from double electrons (either $\beta\beta 0\nu$ or $\beta\beta 2\nu$) by the energy of the blobs defining the beginning and end of the track. As shown in Figure 5, the energy of the blobs is roughly the same (and large), for signal events, while in background events, one of the blobs has an energy smaller than the other. We call this topological criterium of separating signal and background the **blob signature**.

The physics mechanism behind the blob signature is energy deposition in the gas, which acts as a calorimeter. On the other hand, a second topological signature can be implemented by the addition of a moderate, uniform, magnetic field, $B = B_z$, pointing along the TPC axis.

In the presence of such a field both of the emitted electrons in a $\beta\beta 0\nu$ (or a $\beta\beta 2\nu$) decay, should spiral around the field lines in circular motion with radius $r = p_T/B$, where p_T is the momentum of the electron transverse to the direction of the field. A single energetic electron should produce a clear single spiral with radius indicative of its momentum, and a double-electron track with the same energy will produce two spirals each with much less momentum. This information provides an additional way of separating single-electrons arising from background processes from double electrons produced in $\beta\beta$ decays, **in spite of the large multiple scattering that the electrons suffer in a dense HPXE**.

An electron travelling through dense xenon gas undergoes several large-angle scatters that sharply divert an otherwise relatively smooth path through the detector. However, multiple scattering can be incorporated as a noise process, using (for example) the mathematical technique known as the Kalman

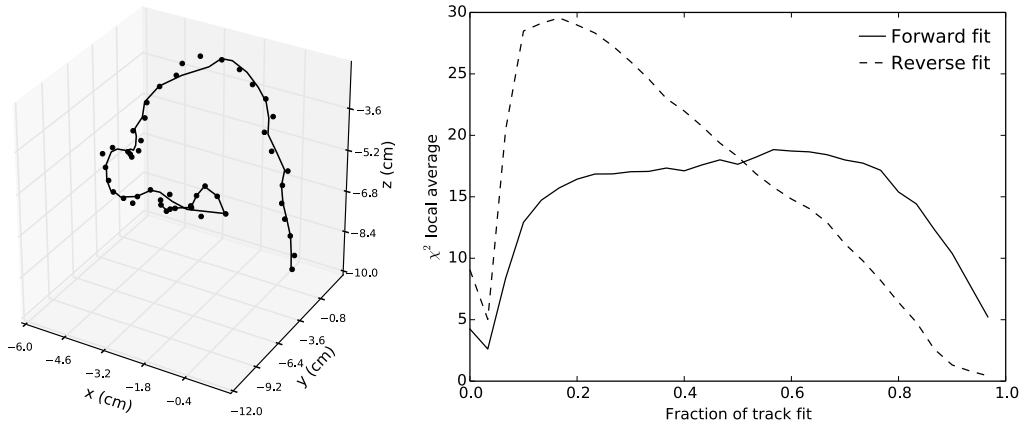


Figura 10: A Kalman Filter fit to a simulated (1 mm resolution) single-electron track in the proper direction of momentum flow. (Right) The local χ^2 values produced along different points of the proper (“forward”) and improper (“reverse”) fits, averaged over 10^4 single-electron tracks. Since the initial momentum is assumed to be the same in both fits, the χ^2 value is artificially high at the beginning of the reverse fit (low multiple scattering error assumed, high multiple scattering found) and artificially low at the end (high multiple scattering error assumed, low multiple scattering found).

Filter²². One can, then, perform fits to reconstructed electron tracks in both directions, **assuming they are single-electron tracks with initial momentum corresponding to the kinetic energy released in $\beta\beta 0\nu$** , obtaining different results for single and double-electron tracks, as illustrated in Figure 10. For single-electron tracks, the fit should perform well in one direction (from the production vertex to the end vertex, since in this case the fit hypothesis is correct) and poorly in the other direction (from end vertex to production vertex, since now the hypothesis is totally wrong, and the electron has, as the start of the fit, vanishing momentum). For double-electron tracks, the fit should fail in both directions.

The illustrative result displayed in Figure 10²³ shows how the “forward fit” (from production to end vertex), differs from the “reverse fit” (from end vertex to production vertex), *even in the absence of a magnetic field*. The right panel of the figure displays the local χ^2 at each step of the fit. In the case of the forward fit (correct hypothesis), the fit converges rapidly to a flat value, since the Kalman Filter keeps updating the momentum of the electron as it losses energy by ionisation. Since the Kalman Filter model incorporates multiple scattering, the trajectory of the electron can indeed be followed, as shown in the left panel of the figure. Instead, the local χ^2 for the reverse fit is too high at the beginning of the fit (the hypothesis is that the momentum is large, when in fact is is very small, therefore the predicted multiple scattering error is underestimated) and too small at the end of the fit (where the situation is reversed and thus the predicted multiple scattering error is overestimated).

In the simulation, the assumed point-error is 1 mm. Such a resolution is difficult to achieve in NEXT-100, unless some additive to reduce the transverse diffusion is added. However, when a solenoidal magnetic field is added the $E \times B$ effect reduces the lateral diffusion to negligible levels for any reasonable value of the field ($B = 0,1$ Tesla is used for the simulations). In NEXT-100, position is reconstructed using SiPMs spaced at a pitch of 10 mm, yielding a resolution (if one would not make use of the SiPM recorded charge to weight the event position) of 3 mm, which improves to ~ 1 mm when the position is weighted by the SiPM recorded charge. Therefore, the resolution assumed in the plot is correct in the presence of a magnetic field (it could also be achieved adding suitable additives such as TMA).

To further enhance the topological signature of NEXT (see Figure 5), one performs a Kalman Fit to double-electron candidates (that is, those which have passed the selection cut requiring that the energy of the two blobs defining the beginning and end of the track is large). As noted, in true signal events, the momentum in each blob vanishes (each blob corresponds to the end-vertex of one of the two electrons emitted in a $\beta\beta$ decay). Instead, in background events managing to “fake” a blob at the start of the track, the fit will succeed in one direction (when we start from the fake blob, in which case the momentum is 2.3

²² A. Cervera-Villanueva, J. J. Gomez-Cadenas y others. En: *Nucl.Instrum.Methods A*. 486 (2002), pág. 639.

²³ J.J. Gomez-Cadenas, J. Renner, A. Cervera, J.A. Hernando, A. Imzaylov, F. Monrabal and J. Muñoz, “Enhancing the topological signature of an HPXe detector by means of a magnetic field”, in preparation.

MeV, corresponding to the kinetic energy of $Q_{\beta\beta}$), and will fail in the other (when we start from the true blob, where the momentum vanishes). Thus, fitting the candidates surviving the blob signature, *under the hypothesis that they are background electrons*, provide an extra rejection criteria. We fit the trajectory of the electron starting from both ends, and accept it only if the fit is consistent, in both cases, with a reverse fit. This simple approach yields a factor 5 extra rejection (for 90% signal efficiency), *in the absence of a magnetic field*.

Indeed, the rejection in the absence of magnetic field comes from an *indirect* measurement of the momentum of the electrons through their multiple scattering angle θ_0 :

$$\theta_0 = \frac{13,6}{\beta c p} \sqrt{\frac{x}{X_0}} + (1 + 0,038 \log \frac{x}{X_0}) \quad (3)$$

where X_0 is the radiation length of the dense xenon gas $\sim P \times 8,48 \text{ g} \cdot \text{cm}^{-2}$ where P is the pressure of the gas) βc is the velocity of the electron and p its momentum.

When a magnetic field B is added the (transverse) momentum of the electrons can be directly measured, $p_T = r \times B$. The determination of p_T does not need to be accurate (which is fortunate, given the fact that the trajectory of the electrons is smeared by multiple scattering), because one relies in the strategy described above. Single (background) electrons will yield a good forward fit (where now the momentum of the electron must be consisted with the track curvature) and a bad reverse fit. Double (signal) electrons will yield reverse fits in two directions. Indeed, for candidate signal (double) electrons is possible to scan the starting point of the reverse fit in both directions, until a good forward fit is found. This corresponds to the vertex of the double electron. We call the topological signature based in the measurement of the momentum of the track (either indirectly or with the aid of a magnetic field) the **vertex signature**.

Work is in progress to assess the final rejection factor and efficiency obtained when a magnetic field (of about ~ 0.1 Tesla) is added and blob and vertex signatures are combined. Our preliminary studies indicate that the combination of both topological signatures will provide a factor of 10 extra rejection of backgrounds at little cost (90%) to the signal efficiency.

The current (estimated) rejection factor for NEXT-100 is 0.4 counts per ton and keV in a year. If a resolution of $Q_{\beta\beta}$ of 0.5% FWHM is confirmed in the large detector as we expect, this translates into 5 counts per ton in the ROI. The addition of a magnetic field may yield a value of 0.5-1 counts per ton in the ROI, thus allowing the HPXe technology to operate in the ton regime without being background limited.

D.2. Barium Tagging

As originally suggested by Moe²⁴, a promising possibilities to further reduce the background is to develop the HPXe technology to unambiguously tag the barium ion produced in the xenon decay, $\text{Xe} \rightarrow \text{Ba}^{++} + 2e^-$. The conceptual idea to tag Ba^+ is illustrated in Figure 9. A “blue” laser of wavelength 493.54 nm excites (“pumps”) the S state, inducing $S \rightarrow P$ transitions, with a lifetime of ~ 10 ns. About 30% of the times the $^2P_{1/2}$ states decay to the state $^2D_{3/2}$, emitting “red” (649.76 nm) fluorescence in a characteristic time of 30 ns. The state $^2D_{3/2}$ is metastable, but a second laser of suitable wavelength (4.1 μm) can be used to induce the transition to the ground state (this is known as “deshelving”). The whole cycle takes less than 50 ns, and therefore several millions of red fluorescence photons can be emitted by a single ion.

The practical application of this conceptual idea is by no means easy, and in fact, it has been shown to be extremely difficult in liquid xenon by the work of the EXO collaboration²⁵. However, it may be feasible in a HPXe detector, where a number of fortunate conditions may occur. These conditions are: a) charge reduction of the emitted barium ion, from Ba^{++} to Ba^+ , which can be induced by collisions with xenon atoms, or by the addition of a suitable quencher; b) “trapping” of the barium ion “in situ” by the surrounding Xe atoms, which result in a very low drift velocity for the ion; c) location of the ion, via the reconstruction of the event topology.

All the above needs to be demonstrated with a systematic R&D program, which must also address additional experimental issues such as pressure broadening of the laser, filtering of Rayleigh scattering, and others. The EXO collaboration has carried out extensive research of the potential for Barium Tagging,

²⁴M.K. Moe, “New approach to the detection of neutrinoless double-beta decay”, Physical Review C Rapid Communications 44 (1991) R931.

²⁵M.J. Dolinski, “The Enriched Xenon Observatory: EXO-200 and Ba^+ tagging”. En: *Nucl.Phys.Proc.Suppl.* 229-232 (2012), págs. 124-127.

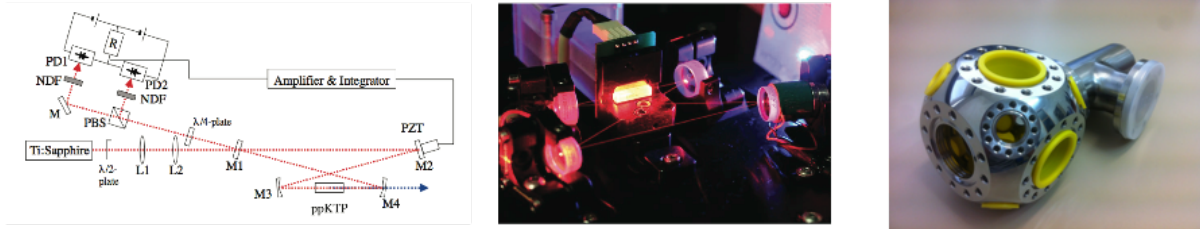


Figura 11: Left: experimental set-up for resonant frequency doubling of a Ti:Sapphire laser using ppKTP. Right: the chamber for the proof-of-concept experiments, built at IFIC, and ready to be installed at CLPU.

not only in a LXe TPC, but also in an HPXE,²⁶. NEXT, on the other hand, has started a collaboration with CLPU²⁷, a Spanish national facility dedicated to ultra-intense lasers, with the aim of carrying out a systematic R&D program to understand the potential of Barium Tagging in a high pressure gas xenon TPC. Such a program involves a set of proof-of-concept experiments, including:

1. **Ba ions generation, phase 1.** Proof-of-principle experiment with Ba ions generated by means of an electrical discharge and/or laser ablation.
2. **Ba ions generation, phase 2.** Proof-of-principle experiment with Ba ions generated by an ion source.
3. **D state deshelling.** A likely scenario is that the collisional induced decay between the metastable state D and the ground state S is either not effective or too slow for obtaining an appreciable fluorescence signal. In this situation the population is trapped in the metastable state D and the fluorescence cycle can not be closed. To avoid this difficulty, deshelling the D state may be needed. A proof-of-principle experiment with an additional laser for deshelling the D state will be performed. The laser needed must have a wavelength of around $4.1 \mu\text{m}$. The alternative, using a red laser would smear the characteristic red fluorescence with scattered photons from the deshelling laser.

Proof of principle experiments

In a first round of experiments we will excite resonantly the $S \leftrightarrow P$ transition of **Ba⁺ ions generated by an electrical discharge** between two barium electrodes and will collect the fluorescence signal of the $P \rightarrow D$ transition (alternatively, laser ablation can be used). Although this generation method is not ideal because several different species other than Ba ions will be generated (e.g., BaO molecules or clusters), it does not need a major technological development.

The laser source needed to resonantly excite the Ba^+ ions must have a wavelength of 493.5 nm, not available in commercial lasers. The laser source will therefore be produced at the CLPU, optimising a tunable Ti:sapphire laser at 987 nm to obtain a second harmonic generation (SHG) at 493.5 nm, see Figure 11. This setup allows the tuning of the wavelength and the control of the bandwidth of the laser, a necessary feature to precisely tune it to the transition frequency (e.g. to correct for pressure broadening and other effects). Fig. 11 also shows the test chamber needed for the experiments. We expect that this initial set of experiments will provide valuable information about the population dynamics in Ba^+ ions, and the influence of the different homogeneous and inhomogeneous broadening mechanisms.

Next, we intent to generate Ba ions by an ion source that will be designed and constructed at the CLPU. This ion source will be based on selective ionisation and mass spectrometry techniques, and it will allow an efficient selection of the desired target species (e.g. Ba^+ and Ba^{++}). With this setup we will be able to study the recombination process $Ba^{++} \rightarrow Ba^+$ and decide whether it can be induced by collisions with xenon atoms, or whether it requires an additive (as demonstrated by). Depending on the results of the experiment, a magnetic trap can be added to improve the experimental conditions.

Finally, we intend to perform a proof of principle experiment with an **additional laser for deshelling the D state**. Our approach will be to use a second laser to induce a two photon transition (one photon is forbidden by selection rules, between the states D and S, see Fig. 9).

²⁶D. Sinclair y col. "Prospects for Barium Tagging in Gaseous Xenon". En: *J.Phys.Conf.Ser.* 309 (2011), pág. 012005.

²⁷URL: <http://www.clpu.es>.

In our program we intend to reproduce and extend the pioneer work of Sinclair and others²⁸, in particular focusing in the scenario of barium-tagging “in situ” (the approach of the EXO R&D appears to be to extract the barium ion, both in the case of liquid and gas detectors). In any case, we believe that the barium tagging program offers a opportunity of joint development with the EXO collaboration.

Clearly the construction of a ton-scale HPXe detector implementing the full Barium Tagging technology is a very challenging enterprise. On the other hand, it appears to be a promising path towards the future.

D.3. NEXT will be BEXT

The addition of either a B-field or Barium Tagging (or both), are clear forward paths to improve the NEXT detector towards the future BEXT²⁹ apparatus, displaying a mass in the range of several tons, with a resolution of 0.5% FWHM and a background rate in the range of 10^{-4} (this appears relatively easy to achieve with a magnetic field) to 10^{-6} (as ultimately possible with barium-tagging) counts/(keV · kg · yr) would be able to fully cover the CRR (and inverted hierarchy) region event in the most pessimistic NME scenario.

E. Conclusions

We have described the current status and the prospects of NEXT. The experimental technique is based in the use of high pressure xenon TPCs with EL readout³⁰. The NEXT-100 detector implements such concept in an asymmetric TPC with PMT-based energy plane and SiPM-based tracking plane³¹. The DEMO and DBDM prototypes have demonstrated excellent energy resolution and the robustness of the topological signature. The NEW apparatus, a 1:2 scale in size (1:8 scale in mass) of NEXT-100 will be commissioned at the LSC in 2015. The NEXT-100 detector will be commissioned at the LSC in 2017 and will reach a sensitivity in the range of 67 to 187 meV depending on the value of the NME, competitive with all other major experiments of the current generation. The technology of HPXe can be extrapolated to the ton scale, adding extra background rejection through two (not mutually exclusive) paths, namely: a) the addition of a magnetic field; b) barium tagging. In both cases, the resulting apparatus, BEXT, will be able to fully explore the inverse hierarchy.

²⁸Sinclair y col., **seernote** 26.

²⁹B-field Experiment with a Xenon TPC, also Barium-Tagging Experiment with a Xenon TPC

³⁰Nygren, **seernote** 9.

³¹Alvarez y col., “NEXT-100 Technical Design Report (TDR): Executive Summary”, **seernote** 9.